Classification of shallow-water acoustic signals via alpha-Stable modeling of the one-dimensional wavelet coefficients

Michael I. Taroudakis[a)]
Department of Mathematics, University of Crete, Institute of Applied and Computational Mathematics-FO.R.T.H., IACM-FORTH, P.O. Box 1527, 711 10 Heraklion, Crete, Greece

George Tzagkarakis[b)] and Panagiotis Tsakalides[c)]
Department of Computer Science, University of Crete, Institute of Computer Science-FO.R.T.H. ICS-FORTH, P.O. Box 1385, 711 10 Heraklion, Crete, Greece

(Received 19 August 2005; revised 13 December 2005; accepted 13 December 2005)

A novel statistical scheme is presented for the classification of shallow water acoustic signals according to the environmental parameters of the medium through which they have propagated. An efficient way to classify these signals is important for inverse procedures in underwater acoustics aiming at the recovery of the geoacoustic parameters of an oceanic environment, using measurements of the acoustic field due to an acoustic source. An important issue in this procedure is the determination of an efficient "observable" of the acoustic signal (feature extraction), which characterizes the signal in connection with the recoverable parameters. The proposed method is based on a transformation of the acoustic signals via a one-dimensional (1D) wavelet decomposition and then by fitting the distribution of the subband coefficients using an appropriate function. We observe that statistical distributions with heavy algebraic tails, such as the alpha-Stable family, are often very accurate in capturing the non-Gaussian behavior of the subband coefficients. As a result, the feature extraction step consists of estimating the parameters of the alpha-Stable model, while the similarity between two distinct signals is measured by employing the Kullback–Leibler Divergence between their corresponding alpha-Stable distributions. The performance of the proposed classification method is studied using simulated acoustic signals generated in a shallow water environment. [DOI: 10.1121/1.2165003]

PACS number(s): 43.30.Pc, 43.60.Pt, 43.60.Lq [AIT] Pages: 1396–1405

I. INTRODUCTION

Among the most interesting inverse problems in underwater acoustics is that of determining the sea-bed or water column parameters from acoustic measurements obtained in the water column. A great amount of literature is devoted to different issues of inversion procedures in underwater acoustics (e.g., Refs. 1–21). Matched-field,[1–7] and modal phase[8–10] inversions are based on measurements made at a number of hydrophones greater than one, whereas ray inversions typical in ocean acoustic tomography[11–13] and modal travel time inversions[14–16] are based on measurements made at a single hydrophone. With the exception of the matched-field techniques, in all other cases a suitable "observable" should be clearly identified. For instance, identification of the modal character of a signal may be based on mode filtering (when multiple receivers are available),[17] on time domain techniques[18] or on techniques utilizing characteristics of the signal in the time-frequency domain.[19–21] The observable is used as the link between the recoverable parameters and the measurements.

All the above mentioned techniques have been the subject of on-going research for the improvement of their performance, in connection with linear or nonlinear inversion procedures, which are necessary for the estimation of a solution to the inverse problem that would be as close to reality as possible. The problem is that the techniques are not always applicable in practical applications (for instance rays or modes may not be identified in a specific experiment), or the sensitivity of the observable to slight changes of the environmental parameters is not always enough for an inversion technique to be applied with confidence and therefore, alternative techniques for signal classification based on a different feature are always in the front of research.

It should be noted that most of the inversion procedures and the associated observable identification (feature extraction) are based on deterministic approaches. The present work concerns signal classification in the case of a single reception, when the available measurement is typically a signal in the time domain. Here, an alternative technique is proposed, in which the tasks of feature extraction (FE) and similarity measurement (SM) are considered in a joint statistical framework. In particular, features that precisely and uniquely describe the internal characteristics of the underwater acoustic signal, are studied taking into account the fact that these features should be sensitive to slight variations of the most important parameters of the environment under consideration. In the proposed approach, the FE step becomes a Maximum Likelihood (ML) estimator of the model parameters fitting the given transformed acoustic signal,

[a)]Electronic mail: taroud@iacm.forth.gr
[b)]Electronic mail: gtzag@ics.forth.gr
[c)]Electronic mail: tsakalid@ics.forth.gr

while the SM step employs the Kullback–Leibler divergence (KLD),[22] which is a statistical measure of similarity between probability density functions having different model parameters. Using this statistical approach each signal is modeled by the marginal densities of the transform coefficients. The above joint statistical framework can then be used in connection with an inversion scheme for the characterization of the ocean environment.

The development of classification schemes in a transform domain is based on the observation that often a linear, invertible transform restructures the signal, resulting in a set of transform coefficients whose structure is simpler to model. For bursty shallow-water acoustic signals, the 1D wavelet transform seems to be a powerful modeling tool, providing a natural arrangement of the wavelet coefficients into multiple scales representing the frequency content of the signal in consecutive bands.[23] Besides, it has been pointed out that the wavelet transforms of bursty signals tend to be sparse, resulting in a large number of coefficients with small magnitude and a small number of large magnitude coefficients.[24] This property gives rise to peaky and heavy-tailed *non-Gaussian* marginal distributions of the wavelet subband coefficients.[24]

The *symmetric alpha-stable* ($S\alpha S$) distributions,[25,26] have proven to be efficient in describing the content of many texture images,[27] which can be considered as of similar type with that of an acoustic signal due to its impulsive character. In the present work, it is demonstrated that this family of distributions is also appropriate for the statistical characterization of a shallow-water acoustic signal. The similarity measurement between two acoustic signals is performed through an appropriate version of the KLD between the corresponding $S\alpha S$ distributions.

The paper is organized as follows: In Sec. II, the mathematical modeling of the source-channel-receiver system is described. In Sec. III, the probabilistic setting for the problem of classifying underwater acoustic signals is briefly reviewed. In Sec. IV, the choice of the univariate symmetric alpha-stable ($S\alpha S$) model for the modeling of the marginal distributions of the wavelet subband coefficients is justified, while the feature extraction as well as the construction of an appropriate similarity measure is described. In Sec. V, the proposed scheme is applied to a database of simulated acoustic signals generated in a shallow-water environment to evaluate the classification performance.

II. MODELING THE SOURCE-CHANNEL-RECEIVER SYSTEM

The acoustic signals to be considered in the present study are simulated broadband tomographic signals modeled using acoustic wave theory applied in shallow water environments. An axially symmetric range-independent environment will be considered.

The acoustic pressure p at a specific location $\mathbf{x}$ for a sound source in location $\mathbf{x}_0$ of frequency ω is given by formula:

$$p(\mathbf{x};\mathbf{x}_0;\omega) = H_{SR}(\mathbf{x};\mathbf{x}_0;\omega)S(\omega), \tag{1}$$

where $H_{SR}(\omega)$ is the system transfer function determined by the Helmholtz equation written in a cylindrical coordinate system (appropriate for the environment under consideration) for a source placed at $r=0$, $z=z_0$;

$$\nabla^2 H_{SR}(r,z;z_0;\omega) + k^2(z)H_{SR}(r,z;z_0;\omega) = -\frac{1}{2\pi r}\delta(r)\delta(z-z_0), \tag{2}$$

supplemented by the appropriate boundary and radiation conditions. $k(z)=\omega/c(z)$ is the wave number, where ω is the circular frequency, and $c(z)$ the sound speed at depth z. $S(\omega)$ is the source excitation function, which is the present study will be considered a Gaussian pulse representing standard types of tomographic signals.

The pressure field in the time domain is given by the inverse Fourier transform:

$$p(r,z;z_0;t) = \mathcal{F}^{-1}[p(r,z;z_0;\omega);\omega\to t] = \frac{1}{2\pi}\int_{-\infty}^{\infty} H_{SR}(r,z;z_0;\omega)S(\omega)e^{i\omega t}d\omega. \tag{3}$$

As in the present study, the analysis is free from any restrictions imposed by the observable, the system transfer function can be calculated using any appropriate propagation model. However, the fact that the environment is considered range independent, a normal mode code is the most accurate for the calculation of the pressure field in the frequency domain and it will be used for the simulation of the acoustic signal.

III. STATISTICAL SIGNAL CLASSIFICATION

In the analysis to follow, signal classification will be associated with an inversion scheme not explicitly defined here, based on minimization of an appropriately defined difference between a measured signal and a signal from a database or from a set of signals simulated from a search space on the environmental parameters to be recovered. The difference has to be determined using a signal feature (or observable). The term "query" used below is in fact the signal to be classified.

Let $\mathcal{F}$ denote the feature space and $\mathbf{X}=\{\mathbf{x}_1,\ldots,\mathbf{x}_N|\mathbf{x}_i \in \mathcal{F}, i=1,\ldots,N\}$ be a set of N independent feature vectors associated to a query. Also, let $\mathcal{S}=\{1,\ldots,K\}$ be the set of class indicators associated with the classes in the database, where each class corresponds to a specific sea environment. Besides, in our setting we consider that each class contains one signal generated with the corresponding environmental parameters. Thus, in the rest of the paper a "class" is equivalent to an environment associated to the corresponding signal in the database. Denote the probability density function (PDF) of the query feature vector space by $p_q(\mathbf{x})$ and the PDF of class $i\in\mathcal{S}$ by $p_i(\mathbf{x})$. The design of a classification scheme in a probabilistic framework, consists of finding an appropriate map $g:\mathcal{F}\mapsto\mathcal{S}$. These maps constitute the set of similarity functions.

The goal of a probabilistic classification system is the

minimization of the probability of classification error, that is, the probability $P(g(\mathbf{X}) \neq s)$. Hence, if we provide the system with a set of feature vectors $\mathbf{X}$ drawn from class $s \in \mathcal{S}$, we want to minimize the probability that the system will classify the query in a class $g(\mathbf{X})$ different from s. It can be shown[28] that the optimal similarity function, that is, the one minimizing $P(g(\mathbf{X}) \neq s)$, is the Bayes or maximum a-posteriory (MAP) classifier

$$g_{\text{opt}}(\mathbf{X}) = arg \max_i P(s=i|\mathbf{X}) = arg \max_i p(\mathbf{X}|s=i)P(s=i), \quad (4)$$

where $p(\mathbf{X}|s=i)$ is the likelihood for the ith class and $P(s=i)$ its prior probability. Under the assumption that all classes are a priori equally likely, the MAP classifier reduces to the ML classifier:

$$g_{\text{opt}}(\mathbf{X}) = arg \max_i p(\mathbf{X}|s=i) \overset{i.i.d.}{=} arg \max_i \frac{1}{N}\sum_{j=1}^{N} \log p(\mathbf{x}_j|s=i). \quad (5)$$

When the number N of feature vectors is large, application of the weak law of large numbers[29] to Eq. (5) results in the following equation:

$$g_{\text{opt}}(\mathbf{X}) = arg \min_i \underbrace{\int p_q(\mathbf{x}) \log \frac{p_q(\mathbf{x})}{p_i(\mathbf{x})} d\mathbf{x}}_{D(p_q\|p_i)}, \quad (6)$$

where $D(p_q\|p_i)$ denotes the KLD or *relative entropy* between the two densities, $p_q(\cdot)$ and $p_i(\cdot)$.

The problem of classifying a given query signal can be formulated as a *hypothesis problem*. The query signal S_q is represented by a feature data set, $\mathbf{X}=\{x_1,\ldots,x_N\}$, obtained after a transformation step, and each class in the database, $S_i(i=1,\ldots,C)$, is assigned with a hypothesis H_i. Therefore, the problem of classifying S_q in one of the database classes, and thus recovering the environmental parameters corresponding to this class, consists of selecting the class in the database that is closer in terms of best hypothesis to the data $\mathbf{X}$ of the given query signal S_q.

Under the assumption that all hypotheses are a priori equally likely, which is equivalent to assume that all values from a predefined search space are equally possible, the optimum rule resulting in the minimum probability of classification error, is to select the hypothesis with the highest likelihood among the C. Thus, the selected class corresponds to the hypothesis, H_{i_1} for which

$$p(\mathbf{X}|H_{i_1}) \geqslant \cdots \geqslant p(\mathbf{X}|H_i), \quad i \neq i_1.$$

A computationally efficient implementation of this setting is to adopt a *parametric* approach. Then, each conditional PDF, $p(\mathbf{X}|H_i)$ is modeled by a member of a family of PDFs, denoted by $p(\mathbf{X};\boldsymbol{\theta}_i)$, where $\boldsymbol{\theta}_i$ is a set of model parameters to be specified. In this framework, the extracted signature for the signal S_i is the *set of estimated model parameters* $\hat{\boldsymbol{\theta}}_i$, computed in the FE step. Then, implementation of Eq. (6) gives the optimal rule for classifying the given query signal S_q to the closest class:

(1) Compute the KLDs between the query density $p(\mathbf{X};\boldsymbol{\theta}_q)$ and the density $p(\mathbf{X};\boldsymbol{\theta}_i)$ associated with class S_i in the database, $\forall i=1,\ldots,C$:

$$D(p(\mathbf{X};\boldsymbol{\theta}_q)\|p(\mathbf{X};\boldsymbol{\theta}_i)) = \int p(x;\boldsymbol{\theta}_q)\log \frac{p(x;\boldsymbol{\theta}_q)}{p(x;\boldsymbol{\theta}_i)} dx. \quad (7)$$

(2) Classify S_q in the class corresponding to the smallest value of the KLD.

The KLD in Eq. (7) can be computed using consistent estimators $\hat{\boldsymbol{\theta}}_q$ and $\hat{\boldsymbol{\theta}}_i$, for the model parameters. The ML estimator is a consistent estimator[22] and for the query signal it gives:

$$\hat{\boldsymbol{\theta}}_q = arg \max_{\boldsymbol{\theta}} \log p(\mathbf{X};\boldsymbol{\theta}). \quad (8)$$

A *chain rule*[29] can also be applied, in order to combine the KLDs from multiple data sets. This rule states that the KLD between two joint PDFs, $p(\mathbf{X},\mathbf{Y})$ and $q(\mathbf{X},\mathbf{Y})$, where $\mathbf{X},\mathbf{Y}$ are assumed to be independent data sets, is given by

$$D(p(\mathbf{X},\mathbf{Y})\|q(\mathbf{X},\mathbf{Y})) = D(p(\mathbf{X})\|q(\mathbf{X})) + D(p(\mathbf{Y})\|q(\mathbf{Y})). \quad (9)$$

IV. STATISTICAL MODELING OF WAVELET SUBBAND COEFFICIENTS VIA SYMMETRIC ALPHA-STABLE DISTRIBUTIONS

In the FE step, an acoustic signal is decomposed into several scales through a multiresolution analysis employing the 1D wavelet transform.[24] The energies of the resulting wavelet coefficients identify the content of the signal at each frequency band (scale). The proposed method is based on the accurate modeling of the tails of the marginal distribution of the wavelet coefficients at each subband: The wavelet subband coefficients in various scales are modeled as $S\alpha S$ random variables.

The $S\alpha S$ distribution is best defined by its characteristic function:[30]

$$\phi(t) = \exp(i\delta t - \gamma^{\alpha}|t|^{\alpha}), \quad (10)$$

where α is the *characteristic exponent*, taking values $0<\alpha\leqslant 2$, δ $(-\infty<\delta<\infty)$ is the *location parameter*, and γ $(\gamma>0)$ is the *dispersion* of the distribution. The characteristic exponent is a shape parameter, which controls the "thickness" of the tails of the density function. The smaller the α, the heavier the tails of the $S\alpha S$ density function. The dispersion parameter determines the spread of the distribution around its location parameter, similar to the variance of the Gaussian. A $S\alpha S$ distribution is called *standard* if $\delta=0$ and $\gamma=1$. The notation $X\sim f_{\alpha}(\gamma,\delta)$ means that the random variable X follows a $S\alpha S$ distribution with parameters α,γ,δ.

In general, no closed-form expressions exist for most $S\alpha S$ density and distribution functions. Two important special cases of $S\alpha S$ densities with closed-form expressions are the Gaussian $(\alpha=2)$ and the Cauchy $(\alpha=1)$. Unlike the Gaussian density which has exponential tails, stable densities

have tails following an algebraic rate of decay ($P(X>x) \sim Cx^{-\alpha}$, as $x \to \infty$, where C is a constant depending on the model parameters), hence random variables following $S\alpha S$ distributions with small α values are highly impulsive.

An important characteristic of non-Gaussian $S\alpha S$ distributions is the nonexistence of second-order moments. Instead, all moments of order p less than α do exist and are called the *fractional lower-order moments*. In particular, the FLOM's of a $S\alpha S$ random variable $X \sim f_\alpha(\gamma, \delta=0)$, are given by:[25]

$$E\{|X|^p\} = (C(p,\alpha)\cdot\gamma)^p, \quad 0 < p < \alpha, \tag{11}$$

where

$$(C(p,\alpha))^p = \frac{2^{p+1}\Gamma\left(\frac{p+1}{2}\right)\Gamma\left(-\frac{p}{\alpha}\right)}{\alpha\sqrt{\pi}\Gamma\left(-\frac{p}{2}\right)} = \frac{\Gamma\left(1-\frac{p}{\alpha}\right)}{\cos\left(\frac{\pi}{2}p\right)\Gamma(1-p)}. \tag{12}$$

During the FE step, the $S\alpha S$ model parameters (α, γ) are estimated using the consistent ML method described by Nolan,[31] which gives reliable estimates and provides the tightest confidence intervals.

The 1D orthogonal discrete wavelet transform (DWT) expands a signal using a certain basis, whose elements are scaled and translated versions of a single prototype filter ("mother wavelet"). In particular, at the first stage the DWT decomposes a signal in one low-frequency *approximation* subband and a high-frequency *detail* subband. The decomposition process can then be iterated, with successive approximation subbands being decomposed in turn, so that one signal is broken down into many lower resolution components (dyadic scales). Thus, a signal decomposed in N levels results in $N+1$ subbands, 1 approximation subband and N detail subbands.

There are interesting properties of the wavelet transform[23] that justify its use in the proposed classification system, among them are the following: *Locality* (signal content can be analyzed in a local area), *multiresolution* (signal is decomposed at a nested set of dyadic scales). Because of these properties, the wavelet transforms of impulsive signals tend to be sparse, resulting in a large number of small magnitude coefficients and a small number of large magnitude coefficients. Importantly, this property is in conflict with the Gaussian assumption, giving rise to peaky and heavy-tailed *non-Gaussian* marginal distributions of the wavelet subband coefficients.

In the proposed data modeling, the statistical fitting proceeds in two steps: First, we assess whether the data deviate from the normal distribution and we determine if they have heavy tails by employing normal probability plots.[32] Then, we check if the data is in the stable domain of attraction by estimating the characteristic exponent α directly from the data and by providing the related confidence intervals. As a further stability diagnostics, we employ the amplitude probability density (APD) curves ($P(|X|>x)$) that give a good indication of whether the $S\alpha S$ fit matches the data near the mode and on the tails of the distribution.

TABLE I. The shallow water environment.

Water depth (H)	200 m
Range (R)	5 km
Central frequency (f_0)	100 Hz
Bandwidth (Δf)	40 Hz
Source/receiver depth	100 m
Sound speed profile in the water:	
$c_w(0)$	1500 m/s
$c_w(\min)$	1490 m/s
$c_w(H)$	1515 m/s
d [depth of min $c_w(z)$]	50 m
Semi-infinite substrate:	
c_{sb}	1600 m/s
ρ_{sb}	1200 kg/m^3

In the subsequent analysis, the effectiveness of a $S\alpha S$ density function for the approximation of the empirical density of the subband coefficients, near the mode and on the tails, is assessed using the signal of Fig. 4(a), which has been simulated using the environmental parameters of Table I. A description of the sea environment corresponding to these environmental parameters will be given in Sec. V.

Figure 1 compares the $S\alpha S$ and generalized Gaussian density (GGD) fits together with the empirical curve for the subbands of the simulated acoustic signal, which was decomposed in three levels using Daubechies' 4 (db4) wavelet.[33] Clearly, the $S\alpha S$ density is superior to the GGD, following more closely both the mode and the tail of the empirical APDs (that is, the APDs where $P(|X|>x)$ is computed as the percentage of the wavelet coefficients with amplitude greater than x, with x varying between 0 and a maximum value

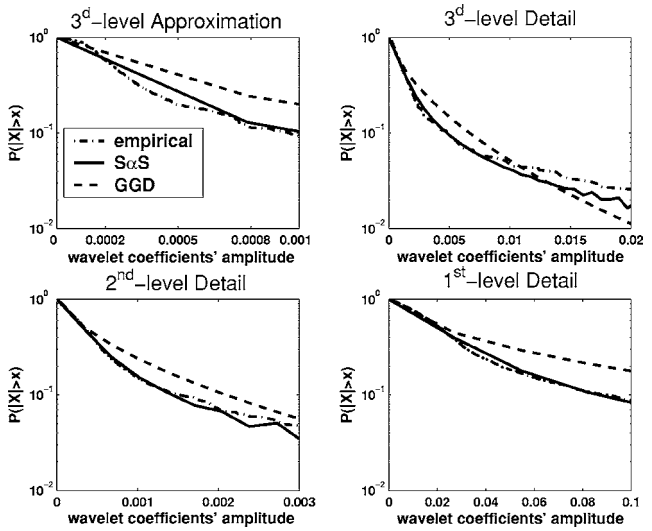

FIG. 1. Modeling of the four wavelet subbands of the three-level decomposition of the *Signal-1* with the $S\alpha S$ and the GGD APD's depicted in solid and dashed lines, respectively. The dashed-dotted line denotes the empirical APD.

TABLE II. $S\alpha S$ modeling of detail subband coefficients of 10 time-domain signals, $\{TD_l\}_{l=20:5:65}$, simulated using the environment of Table I, with $d=l$ m, using Daubechies' 4 wavelet and three decomposition levels. ML parameter estimates and 95% confidence intervals for the characteristic exponent α are given.

	Detail wavelet subbands		
Signal	Level 1	Level 2	Level 3
TD_{20}	1.1792±0.046	1.2104±0.073	1.2119±0.101
TD_{25}	1.1854±0.047	1.2017±0.073	1.1914±0.100
TD_{30}	1.1891±0.048	1.1959±0.075	1.1604±0.102
TD_{35}	1.199±0.048	1.2211±0.074	1.1864±0.102
TD_{40}	1.2031±0.047	1.2159±0.074	1.2294±0.109
TD_{45}	1.2011±0.047	1.1974±0.075	1.1897±0.106
TD_{50}	1.2056±0.046	1.2024±0.075	1.2054±0.104
TD_{55}	1.1978±0.046	1.1978±0.074	1.2503±0.105
TD_{60}	1.2017±0.047	1.2043±0.074	1.2267±0.104
TD_{65}	1.2086±0.047	1.2053±0.073	1.2164±0.103

determined as the maximum amplitude of the available set of wavelet coefficients), than the exponentially decaying GGD. Table II shows the ML estimates of the characteristic exponent α together with the corresponding 95% confidence intervals, for a set of ten simulated acoustic signals obtained using the environment shown in Table I, with d ranging from 20 m to 65 m in steps of 5 m ($d=20:5:65$ m).

Each of them is decomposed in three levels using db4 filters. It can be observed that the confidence intervals depend on the decomposition level. In particular, they become wider as the level increases since the number of samples used for estimating the $S\alpha S$ parameters gets smaller because of the subsampling that takes place between scales. Table II also demonstrates that the coefficients of different subbands exhibit various degrees of non-Gaussianity. Figure 2 displays the histograms of the estimated characteristic exponent values for the simulated acoustic signals in the database to be described in Sec. V, which are also decomposed in three levels using the db4 wavelet, resulting in four wavelet subbands. It is observed that for this set of signals, the wavelet coefficients follow statistics that are highly non-Gaussian and heavy tailed, since the values of the characteristic exponent range in the interval [1,1.4] for each of the subbands. On the other hand, the dispersion γ, with respect to the whole database, ranges in the interval $[10^{-4}, 1.33]$.

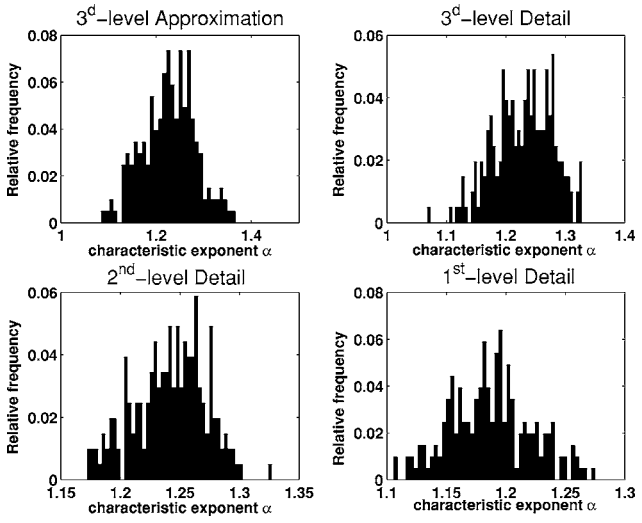

FIG. 2. Histograms representing the relative frequencies of the estimated characteristic exponent values for the 1207 simulated acoustic signals in our database (cf. Sec. V).

A. Feature extraction

After the implementation of the 1D wavelet transform, the marginal statistics of the coefficients at each decomposition level are modeled via a $S\alpha S$ distribution. Then, to extract the features, we simply estimate the (α, γ) pairs at each subband.

Thus, for a given acoustic signal S, decomposed in L levels, its signature is given by the set of the $L+1$ pairs of the estimated parameters:

$$S \mapsto \{(\alpha_1, \gamma_1), (\alpha_2, \gamma_2), \ldots, (\alpha_{L+1}, \gamma_{L+1})\}, \tag{13}$$

where (α_i, γ_i) are the estimated model parameters of the i-th subband. Note that we follow the convention that $i=1$ corresponds to the Detail subband at the first decomposition level, while $i=L+1$ corresponds to the Approximation subband at the L-th level. The total size of the above signature equals $2(L+1)$ which means that the content of an acoustic signal can be represented by only a few parameters, in contrast with the large number of the transform coefficients.

B. Similarity measurement

In the proposed classification scheme, the similarity measurement between two distinct acoustic signals was carried out by employing the KLD. Unfortunately, there is no closed-form expression for the KLD between two general $S\alpha S$ distributions which are not Cauchy or Gaussian. To address this problem, numerical methods could be employed for the computation of the KLD between two numerically approximated $S\alpha S$ densities, resulting in an increased computational burden.

In order to avoid the increased computational complexity of a numerical scheme, first the corresponding characteristic functions are transformed into valid probability density

functions and then the KLD is applied on these normalized versions of the characteristic functions. Due to the one-to-one correspondence between a $S\alpha S$ density and its associated characteristic function, it is expected that the KLD between normalized characteristic functions will be a good similarity measure between the acoustic signals.

If $\phi(\omega)$ is a characteristic function corresponding to a $S\alpha S$ distribution, then the function

$$\hat{\phi}(\omega) = \frac{\phi(\omega)}{c} \tag{14}$$

is a valid density function when

$$c = \int_{-\infty}^{\infty} \phi(\omega) d\omega.$$

For the parameterization of the $S\alpha S$ characteristic function given by Eq. (10), and assuming that the densities are centered at zero, that is $\delta=0$, which is true in the case of wavelet subband coefficients since the average value of a wavelet is zero, the normalization factor is given by

$$c = \frac{2\Gamma\left(\frac{1}{\alpha}\right)}{\alpha\gamma}. \tag{15}$$

By employing the KLD between a pair of normalized $S\alpha S$ characteristic functions, the following closed form expression[27] is obtained:

$$D(\hat{\phi}_1 \| \hat{\phi}_2) = \ln\left(\frac{c_2}{c_1}\right) - \frac{1}{\alpha_1} + \left(\frac{\gamma_2}{\gamma_1}\right)^{\alpha_2} \cdot \frac{\Gamma\left(\frac{\alpha_2+1}{\alpha_1}\right)}{\Gamma\left(\frac{1}{\alpha_1}\right)}, \tag{16}$$

where (α_i, γ_i) are the estimated parameters of the characteristic function $\phi_i(\cdot)$ and c_i is its normalizing factor. It can be proven that $D(\hat{\phi}_1 \| \hat{\phi}_2) \geq 0$ with equality if and only if $(\alpha_1, \gamma_1) = (\alpha_2, \gamma_2)$. That is, the KLD between two signals is minimized when their $S\alpha S$ model parameters are equal.

Thus, the implementation of an L-level DWT on each underwater acoustic signal, results in its representation by $L+1$ subbands, $(D_1, D_2, \ldots, D_L, A_L)$, where D_i, A_i denote the ith level detail and approximation subband coefficients, respectively. Assuming that the wavelet coefficients belonging to different subbands are independent, Eq. (9) yields the following expression for the overall distance between two acoustic signals S_1, S_2:

$$D(S_1 \| S_2) = \sum_{k=1}^{L+1} D(\hat{\phi}_{S_1,k} \| \hat{\phi}_{S_2,k}). \tag{17}$$

V. CLASSIFICATION RESULTS USING SYNTHETIC DATA

In this section, the efficiency of the proposed classification scheme for shallow water acoustic transmissions is evaluated using simulated signals, based on the environment described in Table I. Figure 3 shows the sea environment of the experimental setup, which is assumed range independent and axially symmetric. It consists of a shallow water layer and a semi-infinite bottom (the substrate), which are considered fluid and the sound speed profile may vary with depth in the water layer, while it is constant in the substrate. For simplicity, the density of both layers is assumed to be constant.

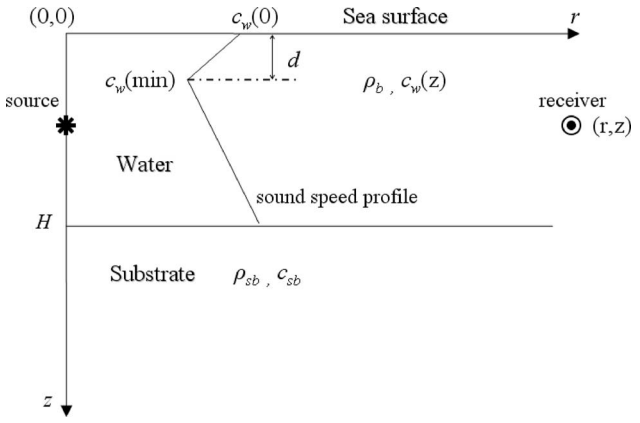

FIG. 3. The shallow water sea environment used in the present study.

The tomographic signals are modeled in the frequency domain using a Gaussian pulse of central frequency $f_0 = 100$ Hz and a bandwidth $\Delta f = 40$ Hz placed at the depth of 100 m. The environmental parameters appear in Table I. First, we generate a set of synthetic signals in order to study the sensitivity of the proposed scheme for small variations of the sound speed in the water column. In particular, for the parameter d, denoting the depth of the minimum sound speed in the water column, a variation in the range $[20, 100]$ m with a step size of 5 m is considered, while the sound speed on the surface varies in the interval $[1495, 1505]$ m/s with a step size equal to 2 m/s and the minimum sound speed at the depth of d m takes values in the interval $[1480, 1500]$ m/s with a step size of 2 m/s. By taking all the permissible combinations of the above parameters according to the sound speed profile shown in Fig. 3, a database with a total of 1207 acoustic signals is obtained, which is equivalent to considering 1207 different sea environments, due to our simulation setup, in which we generate one signal for each setting of the sea parameters. Note that in an actual inversion procedure, the database is never constructed a priori, as more sophisticated algorithms controlling the change of the candidate parameters are applied. However, for the objective of the present study, the construction of the data base using predefined values of the possible environmental parameters is the most appropriate procedure.

The simulated data correspond to measurements at the depth of 100 m and range of 5 km from the source. The data are calculated using the normal-mode program MODE1 developed at FO.R.T.H. These data are provided as input to the inverse discrete Fourier transform to yield the signals in the time domain.

Each of the time-domain signals is decomposed by implementing a three-level 1D DWT using the db2 and db4 wavelets, which have shown the best performance among the wavelets tested for this application. Before proceeding, the APD curves corresponding to the the 4 wavelet subbands of

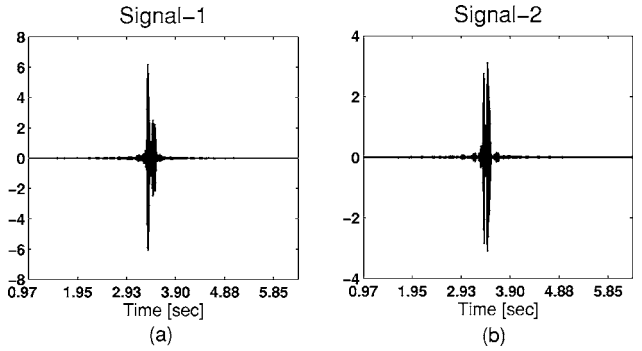

FIG. 4. Acoustic signals simulated in the shallow water environment of Table I with sound speed profiles: (a) $\{c_w(0)=1500\ \mathrm{m/s},\ c_w(\min)=1490\ \mathrm{m/s},\ d=50\ \mathrm{m}\}$ and (b) $\{c_w(0)=1500\ \mathrm{m/s},\ c_w(\min)=1495\ \mathrm{m/s},\ d=50\ \mathrm{m}\}$.

the two signals "Signal-1" and "Signal-2," shown in Fig. 4, are compared (Fig. 5). Note that Signal-1 corresponds to the parameters of Table I, whereas Signal-2 corresponds to $c_w(\min)=1495$ m/s, that is, to a small variation of the minimum sound speed in the water column. It is observed that, although the two signals only slightly differ with the minimum sound speed, their corresponding APDs are clearly distinguishable, especially for the approximation subband and the second-level detail subband, verifying the sensitivity of the $S\alpha S$ model to small variations of the environmental parameters.

In the sequel, the query is the Signal-1. We evaluate the performance of the classification scheme which employs the signatures $\{(\alpha_1,\gamma_1),\ldots,(\alpha_8,\gamma_8)\}$ containing the estimated $S\alpha S$ parameters of the four subbands, as well as the reduced signatures $\{(\alpha_1,\gamma_1),\ldots,(\alpha_6,\gamma_6)\}$ containing the estimated model parameters of the three detail subbands only. The second signature is justified by the fact that the approximation subband, which is a low-pass residual of the original signal, may not preserve the sparsity property of the wavelet transform mentioned above, which results in estimated characteristic exponent values very close or equal to 2, that is the marginal distribution of the approximation subband coefficients is Gaussian.

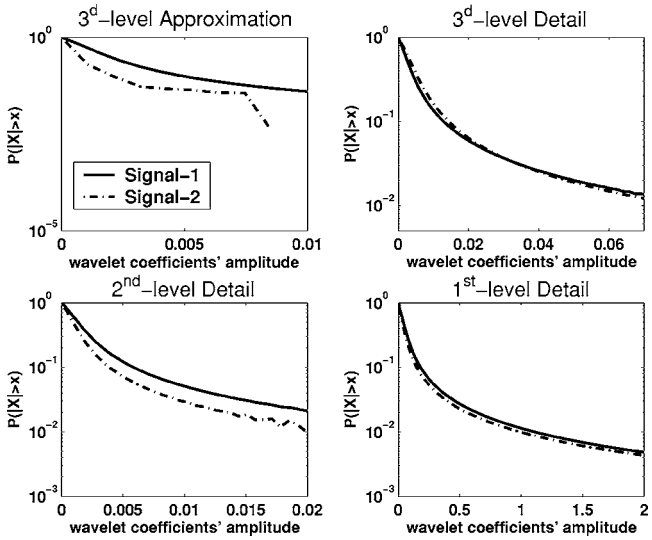

FIG. 5. Comparison between the APD curves of the 4 wavelet subbands for the Signal-1 depicted in solid line and the Signal-2 depicted in dash-dotted line.

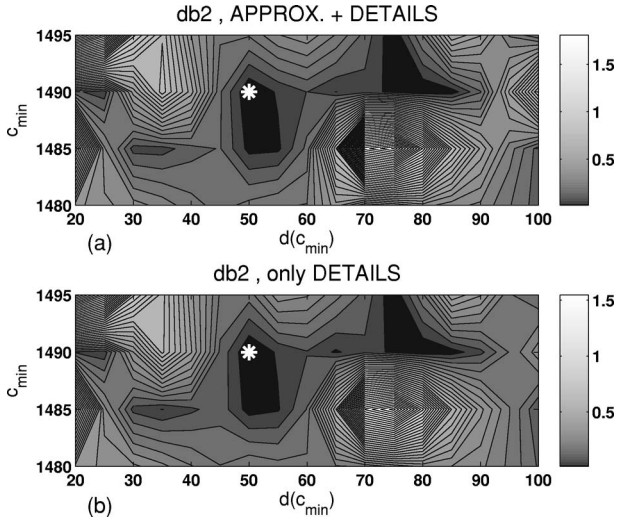

FIG. 6. KLD between Signal-1 and the database signals, decomposed in 3 levels with db2, as a function of $c_w(\min)$ and d using (a) all wavelet subbands and (b) only the details.

Figure 6 displays the KLD between Signal-1 and each signal in the database, as a function of the environmental parameters $c_w(\min)$ and the depth d, where the sound speed takes its minimum value. All of the signals are decomposed using the db2 wavelet. It is observed that in this case, the use of the two signatures—the original [Fig. 6(a)] and the reduced [Fig. 6(b)]—does not change the regions where the minimum KLD is achieved. The star in the two plots corresponds to zero KLD, that is, its coordinates are equal to the environmental parameters of Signal-1 and this point is unique according to what it has already been mentioned about the KLD between $S\alpha S$ characteristic functions.

It can also be seen that the inclusion of the approximation subband only affects the discrimination power of the KLD between the query signal and the signals which are already "far" from it. Note that the maximum KLD occurs in the same region of the two plots, but it takes a higher value (1.8) when the signature contains the $S\alpha S$ parameters of the approximation subband. On the other hand, taking into account this subband during the similarity measurement step, does not benefit the discrimination power of the KLD in the regions, where it is minimized using only the detail subbands. Besides, this wavelet seems to be unsuitable for an efficient classification scheme, since the regions of minimum KLD are quite large and cover different ranges of the two environmental parameters.

Figure 7 presents the KLD between Signal-1 and each signal in the database, as a function of the same two environmental parameters, $c_w(\min)$ and d, when all the signals are decomposed using the db4 wavelet. The improvement, in comparison with the results provided by the db2 wavelet, is obvious. The regions of minimum KLD have been significantly shrunk around the point of zero KLD, denoted by the star, and close to it.

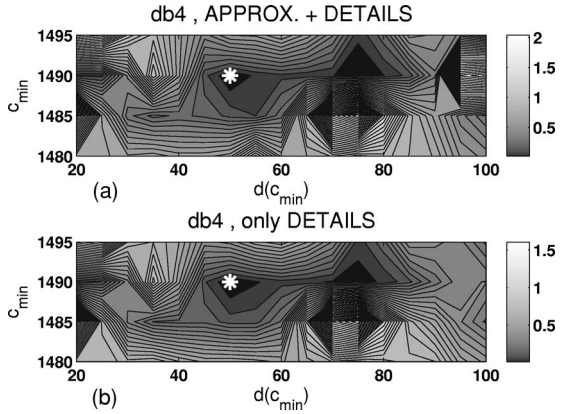

FIG. 7. KLD between Signal-1 and the database signals, decomposed in 3 levels with db4, as a function of c_w(min) and d using (a) all wavelet subbands and (b) only the Details.

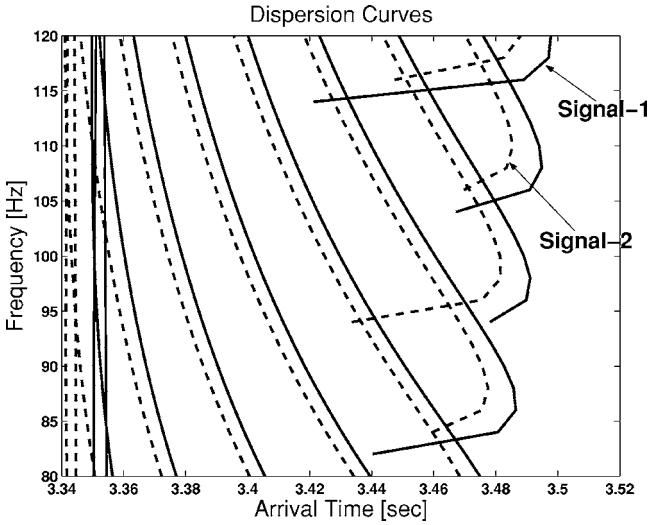

FIG. 8. Dispersion curves corresponding to the simulated signals Signal-1 and Signal-2.

Regarding the comparison with respect to the two signatures, it is observed that the original signature [Fig. 7(a)], containing the $S\alpha S$ parameters of the four subbands, results in a KLD with an increased discrimination power, than the reduced signature [Fig. 7(b)] with the estimated parameters of the detail subbands only. Note also that the maximum KLD (≈ 2) achieved for the original signature, is greater than the maximum KLD corresponding to the reduced one, as in the db2 case. Thus, in the db4 case, the inclusion of the approximation subband is important for the design of an efficient classification scheme.

In order to obtain some indication on the possible advantages of the proposed method for signal classification with respect to other existing ones, we include Fig. 8 which presents the dispersion curves for the two signals under consideration. For shallow water environments, modal inversion schemes are considered effective for the characterization of the environment. For the case under consideration it is clear that lower-order modes, which play an important role in tomographic inversions for the water column, are not well identified for both signals. Although higher-order modes are well identified and they are different for the two signals, no definite conclusion, as regards the efficiency of an inversion scheme based on modal dispersion curves (or modal travel time), can be derived without further analysis. On the other hand, the proposed classification does not suffer from any restrictions as regards the specific character of the signal feature, and therefore it can be considered as a good alternative to signal classification using modal issues, such as modal phase and modal travel time.

As a second illustration, the sensitivity of the $S\alpha S$ model parameters to small variations of the sound speed in the substrate (c_{sb}), as well as the substrate density (ρ_{sb}) is studied. For this purpose, a second synthetic experiment is performed, by generating a set of simulated signals according to the shallow water environmental parameters shown in Table I. The sound speed in the substrate varies in the interval $[1550, 1650]$ m/s with a step size equal to 5 m/s and the substrate density varies in the interval $[1170, 1240]$ kg/m^3 with a step size equal to 1 kg/m^3, resulting in a set with a total of 1491 synthetic acoustic signals.

Each of the above signals is decomposed by implementing a three-level 1D DWT. We tested different wavelet functions, but we present the results only for the db4 wavelet, that gave the best performance. Table III shows the ML es-

TABLE III. $S\alpha S$ modeling of Detail subband coefficients of ten time-domain signals, $\{TD_{\rho_{sb}}\}_{\rho_{sb}=1180:5:1225}$, simulated using the environment of Table I, with substrate density ρ_{sb}, using Daubechies' 4 filter and 3 decomposition levels. ML parameter estimates for the $(\alpha, \gamma/10^{-4})$ parameter pairs are given.

	Detail wavelet subbands		
Signal	Level 1	Level 2	Level 3
TD_{1180}	(1.1576, 10.564)	(1.2058, 3.426)	(1.2531, 211.73)
TD_{1185}	(1.1589, 10.537)	(1.2095, 3.3433)	(1.2491, 211.01)
TD_{1190}	(1.1604, 10.506)	(1.2155, 3.3493)	(1.2454, 210.39)
TD_{1195}	(1.1667, 10.455)	(1.2088, 3.3264)	(1.2428, 209.58)
TD_{1200}	(1.1688, 10.44)	(1.2147, 3.3247)	(1.2397, 208.85)
TD_{1205}	(1.1689, 10424)	(1.2178, 3.3153)	(1.2381, 208.04)
TD_{1210}	(1.1705, 10.472)	(1.2186, 3.3084)	(1.2351, 207.33)
TD_{1215}	(1.1719, 10.408)	(1.2188, 3.2973)	(1.2326, 206.56)
TD_{1220}	(1.1709, 10.39)	(1.2228, 3.2965)	(1.2328, 205.95)
TD_{1225}	(1.1695, 10.369)	(1.2262, 3.2967)	(1.2324, 205.43)

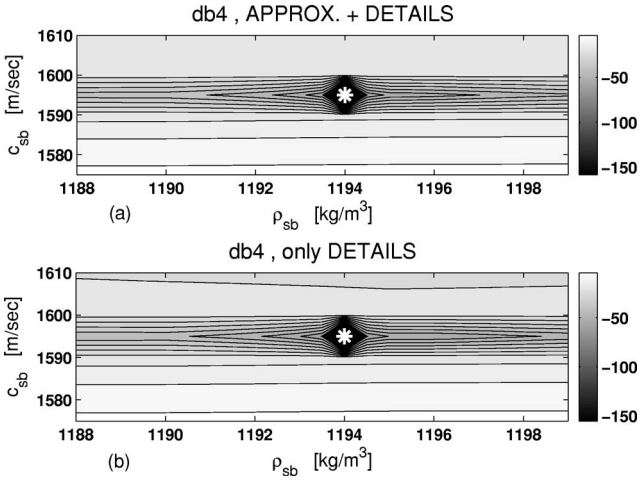

FIG. 9. KLD between the query signal (c_{sb}=1595 m/s, ρ_{sb}=1194 kg/m^3) and the 1491 database signals, decomposed in 3 levels with db4, as a function of c_{sb} and ρ_{sb} using (a) all wavelet subbands and (b) only the details.

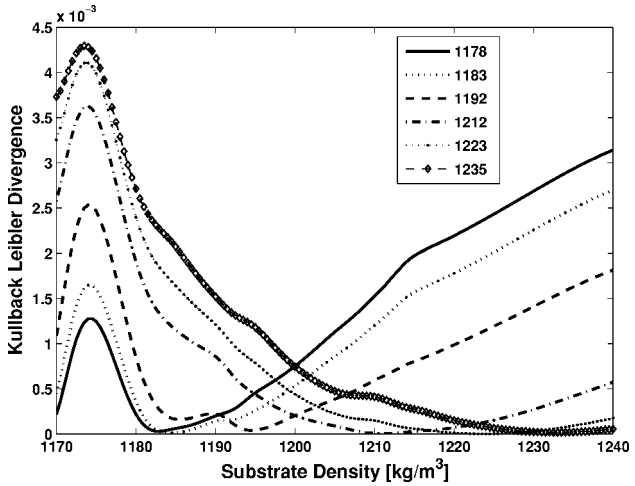

FIG. 10. KLD between each one of the 6 signals, with the same c_{sb} =1600 m/s and ρ_{sb}=1178, 1183, 1192, 1212, 1223 and 1235 kg/m^3, respectively, and the 71 database signals obtained for c_{sb}=1600 m/s and by varying the sediment density in the interval [1170:1:1240] kg/m^3.

timates for the $S\alpha S$ parameter pairs $(\alpha, \gamma/10^{-4})$ for ten signals of the above dataset, with the same sound speed in the substrate (c_{sb}=1600 m/s) and different substrate density taking the values ρ_b=1180:5:1225. It is clear that for these selected signals, the corresponding estimated characteristic exponents α, as well as the estimated dispersions γ are quite close. Thus, one could claim that it would be difficult to classify a given query signal in the correct environment, represented by the database signal whose feature vector is closest to that of the query signal than the feature vectors of the other database signals, since the model parameters corresponding to the wavelet subbands of two different database signals are very close to each other.

However, Fig. 9 displays the KLD between the query, which is the signal corresponding to c_{sb}=1595 m/s and ρ_{sb} =1194 kg/m^3, and each one of the 1491 signals in the database, as a function of the environmental parameters c_{sb} and ρ_{sb}. The values of the KLD are shown in the dB scale and the x,y axes have been properly adjusted, for a better visualization. The region around the location of minimum KLD, denoted by the star in the two plots, is quite tight, indicating a high discrimination power of the KLD between $S\alpha S$ distributions, even in the cases of very small variations of the substrate sound speed and the substrate density. Besides, it is clear that in this case, the use of the original signature [Fig. 9(a)] results in an increased performance compared with the reduced one [Fig. 9(b)].

Figure 10 shows that the proposed classification scheme is able to perform a satisfactory correspondence of a given query to the correct environment, when the substrate density is variable, even in the case that the $S\alpha S$ model parameters are close enough. In particular, each curve in this figure corresponds to the KLD values between each one of the six signals with the same c_{sb}=1600 m/s and different densities ρ_b=1178, 1183, 1192, 1212, 1223, and 1235 kg/m^3, respectively, and the 71 database signals corresponding to c_{sb} =1600 m/s and $\rho_{sb} \in$ [1170:1:1240] kg/m^3. We observe that, for each of the last five signals, the minimum KLD is achieved very close to the corresponding true substrate density, despite the fact that the flatness of the region around the expected density is different for each curve. For the first signal (ρ_{sb}=1178), the difference between the true density and the density that achieves the minimum KLD is slightly larger, but it still remains in a small region on the "substrate density" axis, which is close enough to the true density.

Taking into account the well-known fact, that the density value of the substrate is very difficult to be determined accurately using a typical inversion scheme, this result reinforces our persuasion that a statistical similarity function, such as the KLD, is often preferable than a deterministic one, such as a norm-based distance function between the feature vectors. In addition, it reveals the necessity for the construction of an appropriate similarity function that will be capable of improving the classification performance, even in the cases that the feature extraction results in features that may not be too distinct. The proposed version of the KLD between $S\alpha S$ distributions, seems to be quite powerful with respect to discriminating two simulated acoustic signals with $S\alpha S$ parameters (α, γ) that are very close to each other.

This sensitivity of the KLD to small variations of the sound speed profile in shallow water and the bottom, as well as to small variations of the substrate density, makes this similarity measure an appropriate tool that can be used as the basis of an inversion procedure for geoacoustic inversions.

VI. CONCLUSIONS AND FUTURE WORK

In this paper, the design of a classification scheme for acoustic signals recorded in shallow water, based on a $S\alpha S$ modeling of the coefficients of a 1D wavelet decomposition has been discussed. In particular, it was demonstrated that the set of the parameters of the $S\alpha S$ distributions, describing the statistical behavior of the 1D wavelet subband coefficients, is an effective set of features that can be used for the classification of an underwater acoustic signal. Regarding the task of similarity measurement, the choice of the KLD between normalized $S\alpha S$ characteristic functions, which is a statistical measure of similarity, seems to be appropriate in

capturing the statistical difference of two distinct signals generated even in very similar environments, and thus this KLD is capable in distinguishing two shallow-water environments with approximately the same parameters. This means that the proposed technique can classify, with high probability, an underwater signal in the correct environment where it was recorded. Moreover, it has been shown that the choice of the suitable wavelet function is important for an increased classification performance.

The main computational cost of the proposed scheme, when applied for an inversion problem, is due to the preprocessing step, which includes simulation of a signal in the time-domain using the inverse discrete Fourier transform, followed by the 1D DWT. After this process, the proposed scheme is efficient in terms of computational complexity, since each signal is now represented by only a few parameters, the estimated $S\alpha S$ model parameters. Besides, the KLD has a closed-form expression, which can be simply evaluated using the estimated parameters.

Future research directions, which could further result in an improved classification system with decreased probability of classification error, before a complete inversion procedure is applied for the classification of a sea environment, are the following: First of all, the main assumption throughout the present work was the statistical independence between the wavelet coefficients at adjacent decomposition levels. Regarding the task of similarity measurement between two distinct acoustic signals, we did not take into account the possible interlevel dependencies between the transform coefficients. In this case, we could further improve the power of the similarity measure by considering some kind of chain rule for the KLD between two signals,[22] or by exploiting the possible interdependencies using a multivariate statistical model.

ACKNOWLEDGMENTS

This work was partially supported by the Greek General Secretariat for Research and Technology under Program "THALATTA" and the European Union under Program MC-WAVE.

[1]M. Taroudakis and G. M. Makrakis, (eds.), *Inverse Problems in Underwater Acoustics* (Springer, New York, 2001).
[2]A. Tolstoy, O. Diachok, and L. Frazer, "Acoustic tomography via matched-field processing," J. Acoust. Soc. Am. **89**, pp. 1119–1127 (1991).
[3]A. Tolstoy, *Matched-Field Processing for Underwater Acoustics* (World Scientific, Singapore, 1993).
[4]J. Comput. Acoust. **6**, 1–289 (1998).
[5]S. E. Dosso, M. L. Yeremey, J. M. Ozard, and N. R. Chapman, "Estimation of ocean bottom properties by matched-field inversion of acoustic field data," IEEE J. Ocean. Eng. **18**, 232–293 (1993).
[6]L. Jaschke and N. R. Chapman, "Matched-field inversion of broadband data using the freeze bath method," J. Acoust. Soc. Am. **106**, 1838–1851 (1999).
[7]M. I. Taroudakis and M. G. Markaki, "On the use of matched-field processing and hybrid algorithms for vertical slice tomography," J. Acoust. Soc. Am. **102**, 885–895 (1997).
[8]S. Rajan, J. F. Lynch, and G. V. Frisk, "Perturbative inversion methods for obtaining bottom geoacoustic parameters in shallow water," J. Acoust. Soc. Am. **82**, 998–1017 (1987).
[9]E. C. Shang, "Ocean acoustic tomography based on adiabatic mode theory," J. Acoust. Soc. Am. **85**, 1531–1537 (1989).
[10]M. I. Taroudakis and J. S. Papadakis, "A modal inversion scheme for ocean acoustic tomography," J. Comput. Acoust. **1**, 395–421 (1993).
[11]W. Munk and C. Wunsch, "Ocean acoustic tomography: A scheme for large-scale monitoring," Deep-Sea Res., Part A **26**, 123–161 (1979).
[12]W. Munk, P. Worcester, and C. Wunsch, *Ocean Acoustic Tomography* (Cambridge University Press, Cambridge, UK, 1995).
[13]U. Send *et al.* (The THETIS-2 Group), "Acoustic observations of heat content across the mediterranean sea," Nature (London) **38**, 615–617 (1997).
[14]E. C. Shang and Y. Y. Wang, "On the possibility of monitoring the el niño by using modal ocean acoustic tomography," J. Acoust. Soc. Am. **91**, 136–140 (1992).
[15]M. I. Taroudakis, "A comparison of the modal-phase and modal-travel time approaches for ocean acoustic tomography," in *Proceedings of the 2nd European Conference on Underwater Acoustics*, (edited by L. Bjørnø), pp. 1057–1062 (1994).
[16]M. I. Taroudakis and M. Markaki, "Tomographic inversions in shallow water, using modal travel time measurements," Acta Acust. (Beijing) **87**, 647–658 (2001).
[17]E. L. Lo, J. X. Zhou, and E. C. Shang, "Normal mode filtering in shallow water," J. Acoust. Soc. Am. **74**, 1833–1836 (1983).
[18]M. I. Taroudakis, "Identifying modal arrivals in shallow water for bottom geoacoustic inversions," J. Comput. Acoust. **8**, 307–324 (2000).
[19]G. R. Potty and J. H. Miller, "Geoacoustic tomography: Range dependent inversions on a single slice," J. Comput. Acoust. **8**, 325–346 (2000).
[20]G. R. Potty, J. H. Miller, J. F. Lynch, and K. B. Smith, "Tomographic inversion for sediment parameters in shallow water," J. Acoust. Soc. Am. **108**, 973–986 (2000).
[21]M. I. Taroudakis and G. Tzagkarakis, "On the use of the reassigned wavelet transform for mode identification," J. Comput. Acoust. **12**, 175–196 (2004).
[22]S. Kullback, *Information Theory and Statistics* (Dover, New York, 1997).
[23]S. Mallat, *A Wavelet Tour of Signal Processing* (Academic, New York, 1998).
[24]S. G. Mallat, "A theory for multiresolution signal decomposition: The wavelet representation," IEEE Trans. Pattern Anal. Mach. Intell. **11**, 674–692 (1989).
[25]G. Samorodnitsky and M. S. Taqqu, *Stable Non-Gaussian Random Processes: Stochastic Models with Infinite Variance* (Chapman and Hall, New York, 1994).
[26]C. L. Nikias and M. Shao, *Signal Processing with Alpha-Stable Distributions and Applications* (Wiley, New York, 1995).
[27]G. Tzagkarakis and P. Tsakalides, "A statistical approach to texture image retrieval via alpha-stable modeling of wavelet decompositions," *Proceedings of the 5th International Workshop on Image Analysis for Multimedia Interactive Services, Lisboa, Portugal*, April 21–23, 2004.
[28]K. Fukunaga, *Introduction to Statistical Pattern Recognition* (Academic, New York, 1990).
[29]T. Cover and J. Thomas, *Elements of Information Theory* (Wiley, New York, 1991).
[30]J. P. Nolan, "Parameterizations and modes of stable distributions," Stat. Probab. Lett. **38**, 187–195 (1998).
[31]J. P. Nolan, "Numerical calculation of stable densities and distribution functions," Commun. Stat.-Stochastic Models **13**, 759–774 (1997).
[32]J. Chambers, W. Cleveland, B. Kleiner, and P. Tukey, *Graphical Methods for Data Analysis* (Chapman and Hall, New York, 1983).
[33]C. K. Chui, *An Introduction to Wavelets* (Academic, New York, 1992).